ISSN 1063-7834, Physics of the Solid State, 2011, Vol. 53, No. 3, pp. 510–517. © Pleiades Publishing, Ltd., 2011.
Original Russian Text © E.A. Mikhaleva, I.N. Flerov, V.S. Bondarev, M.V. Gorev, A.D. Vasiliev, T.N. Davydova, 2011, published in Fizika Tverdogo Tela, 2011, Vol. 53, No. 3, pp. 478–484.

FERROELECTRICITY

Phase Transitions and Caloric Effects in Ferroelectric Solid Solutions of Ammonium and Rubidium Hydrosulfates

E. A. Mikhaleva[a, b, *], I. N. Flerov[a, b, **], V. S. Bondarev[a, b], M. V. Gorev[a, b], A. D. Vasiliev[a, b], and T. N. Davydova[b]

[a] *Institute of Engineering Physics and Radioelectronics, Siberian Federal University, pr. Svobodny 79, Krasnoyarsk, 660041 Russia*

* *e-mail: katerina@iph.krasn.ru*

** *e-mail: flerov@iph.krasn.ru*

[b] *Kirensky Institute of Physics, Siberian Branch, Russian Academy of Sciences, Akademgorodok 50, Krasnoyarsk, 660036 Russia*

Received June 24, 2010

Abstract—Structural, calorimetric, dielectric, and electrocaloric investigations of $Rb_x(NH_4)_{1-x}HSO_4$ ferroelectric solid solutions have been performed. It has been found that rubidium atoms inhomogeneously occupy nonequivalent crystallographic positions in the structure $P2_1/c$. The influence of the rubidium concentration on the sequence of phase transitions in the NH_4HSO_4 compound has been established. It has been revealed that the consequences of the Landau theory can be applied to the description of the temperature dependences of the anomalous heat capacity and the electrocaloric effect over a wide range of temperatures. Comparative evaluations of the electrocaloric and barocaloric effects in hydrosulfate and triglycine sulfate crystals have been carried out.

DOI: 10.1134/S1063783411030188

1. INTRODUCTION

In recent years, the electrocaloric, magnetocaloric, and barocaloric effects have attracted increased attention of researchers due to the fundamental and applied aspects of these phenomena. As regards the applied aspects, the case in point is the possibility of using materials having caloric effects in solid-state cooling devices [1, 2]. The cooling technique based on any caloric effect lies in a reversible change in the temperature or entropy of a thermodynamic system (ferroelectric, ferromagnetic, and ferroelastic) in response to external fields (electric, magnetic, and mechanical stresses) under adiabatic or isothermal conditions, respectively, which makes it possible to organize a classical inverse Carnot cycle. For a long time, the magnetocaloric and electrocaloric effects have not attracted special attention, because their magnitudes in materials known by that time were too small in order to provide a high efficiency of refrigeration cycles. However, gradual progress in theoretical and experimental methods of investigation of magnetothermal and electrothermal properties of materials and discovery of new compounds (ferroics), which undergo phase transitions accompanied by significant changes in the entropy, favored the renewal of scientific and practical interest in the study of the magnetocaloric and electrocaloric effects. At present, there exist a wide range of magnets and a rather limited number of ferroelectrics that can be recommended for the use as solid refrigerants [1–3]. Among magnetic materials, large magnitudes of the intensive (ΔT_{ad}) and extensive (ΔS_{ce}) effects are characteristic of perovskite-like manganites, alloys, intermetallic compounds, etc. In the family of ferroelectrics, order–disorder phase transitions, i.e., transitions associated with the large change in the entropy $\Delta S/R > \ln 2$, occur more rarely. The largest electrocaloric effect was observed in lead zirconate titanate thin films, and, only in this form, the material appeared to be competitive in the caloric efficiency with the most promising magnetic solid-state refrigerants [1, 4].

Experimental investigations of the barocaloric effect (BCE), which has long been used in vapor–gas refrigeration cycles, have been started rather recently, and, correspondingly, this effect has been studied to a considerably lesser extent as compared to the magnetocaloric and electrocaloric effects. The technique of adiabatic cooling in the vicinity of the structural phase transition induced by the external pressure in compounds containing rare-earth ions was proposed in 1998 [5]. More recently, investigations of the barocaloric effect in ferroelastics revealed that, at relatively low hydrostatic pressures, fluoroxygen compounds that undergo phase transitions associated with the ordering of cations and anions can be characterized by values of ΔS_{ce} and ΔT_{ad} comparable to the best parameters of the magnetocaloric effect in magnets [6, 7]. It was demonstrated that one of the factors responsible

for the high caloric efficiency of ferroelastic materials is an anomalously large susceptibility of the transition temperatures to the external pressure. It should be noted that the barocaloric effect is more universal as compared to the magnetocaloric and electrocaloric effects, because the pressure can affect subsystems of different physical natures that form the thermodynamic system as a whole. Therefore, the study of the possibility of different caloric effects (electrocaloric, magnetocaloric, and barocaloric) occurring in the same material is of special interest. First, this allows one to obtain additional information on the nature and mechanism of phase transitions, and, second, the simultaneous action of several external fields can be used for increasing a combined caloric efficiency of the material. For example, a strong magnetoelastic coupling leads to an anomalously large magnitude of the magnetocaloric effect in MnAs [8]. To the best of our knowledge, the barocaloric effect in ferroelectrics has never been studied.

This work continues the investigation of the caloric effects in crystals of the hydrosulfate family A^+HSO_4, which was started in our earlier work [9]. It should be recalled that the nature of A^+ cations substantially affects the sequence of structural distortions. The crystal with the NH_4^+ tetrahedral cation undergoes two phase transitions $P2_1/c$ $(T_1) \longrightarrow Pc(T_2) \longrightarrow P\text{-}1$, whereas only one transition $P2_1/c$ $(T_1) \longrightarrow Pc$ occurs in the $RbHSO_4$ crystal [10]. The temperature T_1 and the corresponding change in the entropy $\Delta S_1/R \approx 0.2$ are insignificantly changed upon substitution $NH_4 \longrightarrow Rb$, which made it possible to believe that the SO_4^{-2} anions are responsible for the appearance of the ferroelectric phase Pc. The low-temperature phase transition in the ammonium hydrosulfate is a pronounced first-order transformation with a rather large entropy $\Delta S_2/R \approx 1$. The appearance of the antiferroelectric phase P-1 was attributed to the ordering of ammonium cations by Miller et al. [11] and to the change in the anion orientation in the model proposed in [10]. Until recently, the question regarding the influence of progressive replacement of tetrahedral cations by spherical cations in a number of $Rb_x(NH_4)_{1-x}HSO_4$ solid solutions on (1) the stability of the antiferroelectric phase P-1, (2) the character of change in the entropy at temperatures of phase transitions of different physical natures, and (3) the magnitude of the intensive electrocaloric effect has remained open. Information on the barocaloric effect was absent at all.

The purposes of this work were as follows: (1) to refine the structure and to study the heat capacity, permittivity, T–x phase diagram, and electrocaloric effect in the $Rb_x(NH_4)_{1-x}HSO_4$ compounds with $x = 0$, 0.02, 0.04, and 0.33 and (2) to calculate the magnitudes of the electrocaloric and barocaloric effects for $Rb_x(NH_4)_{1-x}HSO_4$ and triglycine sulfate crystals from the electric equation of state with the use of the data on the heat capacity, permittivity, and entropy, as well as the pressure–temperature phase diagrams.

2. SAMPLE PREPARATION AND EXPERIMENTAL TECHNIQUE

Single crystals of $Rb_x(NH_4)_{1-x}HSO_4$ solid solutions were grown from an aqueous solution of the NH_4HSO_4 and $RbHSO_4$ salts taken in the corresponding ratio. The most perfect crystals were prepared using the growth conditions closest to equilibrium conditions, with a minimum supersaturation of the solution, and at a minimum temperature gradient.

The quality of the grown samples was checked and the refinement of the percentage ratio between Rb^+ and NH_4^+ cations was performed on a Bruker SMART APEX II automatic X-ray diffractometer. It was established that the real rubidium concentrations x_{exp} (0.02, 0.04, 0.33) considerably exceed the concentrations x_{calc} (0.0025, 0.01, 0.10) expected from growth experiments. It can be seen that the difference between these concentrations decreases with an increase in the rubidium concentration.

The most detailed structural investigations were performed for the $Rb_{0.33}(NH_4)_{0.67}HSO_4$ solid solution sample. The initial phase had a monoclinic symmetry with space group $P2_1/c$ ($z = 4$). The reliability factor in the determination of the structural parameters was quite satisfactory: $R_1 = 0.0192$.

The structure refinement revealed that the rubidium atoms occupy two nonequivalent positions existing in the structure in different ratios: Rb1/Rb2 = 0.368/0.292. As will be shown below, the nonuniform distribution of cations resulted in specific features of the behavior of anomalous physical properties in the phase transition ranges.

3. CALORIMETRIC, DIELECTRIC, AND ELECTROCALORIC INVESTIGATIONS

The primary measurements of the heat capacity were carried out on a DSM-10M differential scanning microcalorimeter for the $Rb_x(NH_4)_{1-x}HSO_4$ samples 0.10–0.12 g in weight. The rate of variation in the temperature during heating and cooling was equal to 8 K/min. The high-temperature phase transition in crystals of A^+HSO_4 hydrosulfates is a second-order transformation with a small heat capacity anomaly, which is approximately equal to 10% of the lattice heat capacity. In this respect, we failed to record this transition in the course of the above measurements.

The results of the investigation of the first-order transition at T_2 between the ferroelectric and antiferroelectric phases in the form of the temperature dependences of the excess heat capacity of the solid solutions are presented in Fig. 1. In order to reliably

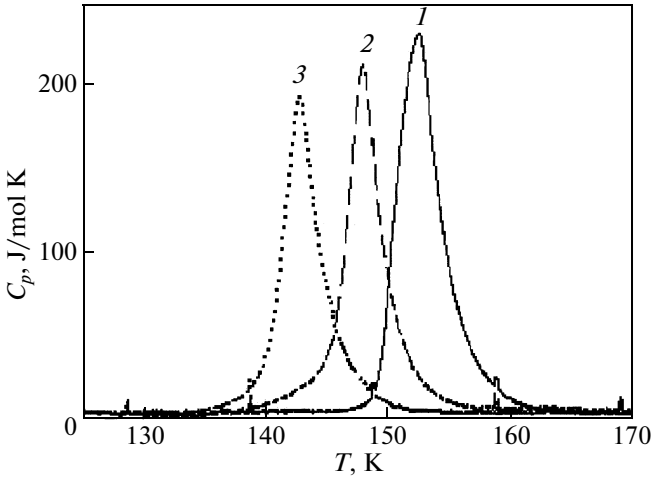

Fig. 1. Temperature dependences of the excess heat capacity in the vicinity of the phase transition $Pc \longrightarrow P\text{-}1$ in the $Rb_x(NH_4)_{1-x}HSO_4$ solid solutions with x = (*1*) 0, (*2*) 0.02, and (*3*) 0.04.

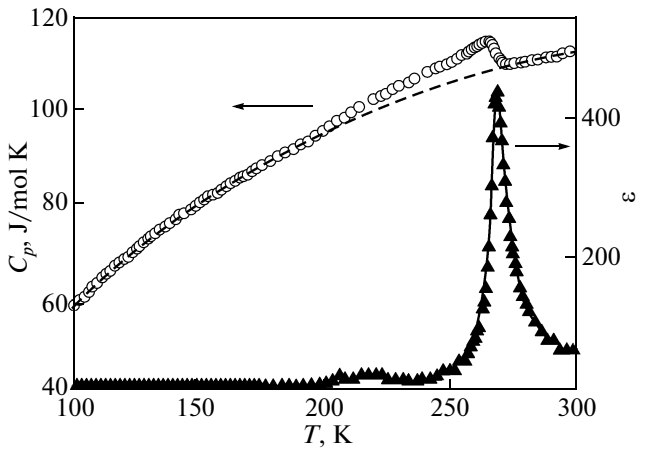

Fig. 2. Temperature dependences of the heat capacity and the permittivity for the $Rb_{0.33}(NH_4)_{0.67}HSO_4$ crystal. The dashed line indicates the lattice heat capacity.

determine the shift in the temperature T_2 and change in the corresponding enthalpy, we also studied the NH_4HSO_4 initial compound. As could be expected, the transition temperature decreases with an increase in the rubidium concentration and, for the crystal with $x = 0.33$, is not observed down to 120 K, i.e., the lower temperature limit of measurements on the DSM calorimeter. At low rubidium concentrations, the dependence $T_2(T)$ is almost linear with the coefficient $dT_2/dx = 2.4$ K/%.

The changes in the enthalpy ΔH_2 (J/mol) and the entropy ΔS_2 (J/mol K) were determined by integrating the functions $\Delta Cp(T)$ and $(\Delta Cp/T)(T)$ and appeared to be as follows: $\Delta H_2 = 1100 \pm 160$ and $\Delta S_2 = 7 \pm 1$ for $x = 0$, $\Delta H_2 = 900 \pm 140$ and $\Delta S_2 = 6.0 \pm 0.9$ for $x = 0.02$, and $\Delta H_2 = 800 \pm 120$ and $\Delta S_2 = 5.6 \pm 0.8$ for $x = 0.04$.

A decrease in these characteristics with an increase in the concentration x is most likely associated with the smearing of the phase transition, in particular, due to the nonuniform distribution of rubidium atoms (revealed in the structural experiments) over nonequivalent crystallographic positions.

The sample of the $Rb_{0.33}(NH_4)_{0.67}HSO_4$ composition was grown in the form of a single crystal with a large volume, which allowed us to measure its heat capacity in an adiabatic calorimeter over a wide range of temperatures in which the sequence of the phase transitions $P2_1/c(T_1) \longrightarrow Pc(T_2) \longrightarrow P\text{-}1$ occurs in the NH_4HSO_4 compound [10]. The sample was cut in the form of a parallelepiped, and silver electrodes were evaporated onto the largest (in area) faces perpendicular to the ferroelectric axis c. This made it possible to perform the measurements for the electrically short-circuited sample, i.e., at $E = 0$. As a result of the measurements (Fig. 2), we recorded only one heat capacity anomaly corresponding to the phase transition between the paraelectric and ferroelectric phases. In parallel, we measured the temperature dependence of the permittivity of the crystal $\varepsilon(T)$ (Fig. 2).

The temperature of the maximum of the heat capacity $T_1(C_{max}) = 265.2$ K turned out to be lower than $T_1(\varepsilon_{max}) = 269.0$ K. The significant difference between these temperatures is associated with the smearing of the heat capacity anomaly, for which, according to [12], the transition temperature in actual fact corresponds to the temperature of the maximum of the derivative dC_p/dT at $T > T_1(C_{max})$. In our case, this temperature is equal to 269.0 ± 0.2 K.

In order to separate the anomalous contribution to the total heat capacity of the sample, it was necessary to determine the lattice heat capacity C_{lat}. For this purpose, the experimental data $C_p(T)$ far from the temperature T_1 were approximated by both a polynomial function and a combination of Debye and Einstein functions. Both variants led to results that are in satisfactory agreement with respect to the form of the dependence $C_{lat}(T)$. The maximum value of the anomalous heat capacity for the sample under investigation was approximately equal to 5.6% of the lattice heat capacity C_{lat}. Above the temperature T_1, the excess heat capacity was observed over a considerably wider range of temperatures as compared to that for the ammonium and rubidium hydrosulfates [10, 13]. Certainly, one of the factors responsible for this phenomenon is the nonuniform distribution of rubidium atoms over nonequivalent crystallographic positions, which was revealed in the X-ray diffraction investigations (see Section 2) and results in the smearing of anomalies of physical properties.

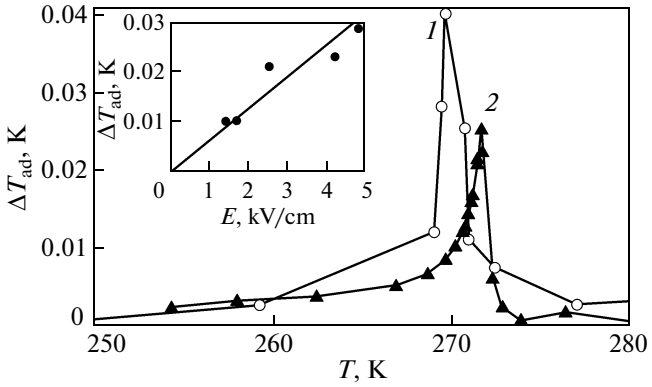

Fig. 3. Temperature dependences of the magnitude of the intensive electrocaloric effect in the range of the transition $P2_1/c \longrightarrow Pc$ for (*1*) $Rb_{0.33}(NH_4)_{0.67}HSO_4$ at E = 3.4 kV/cm and (*2*) NH_4HSO_4 at E = 1.5 kV/cm [9]. The inset shows the dependence $\Delta T_{ad}(E)$ for $Rb_{0.33}(NH_4)_{0.67}HSO_4$ at T = 269 K.

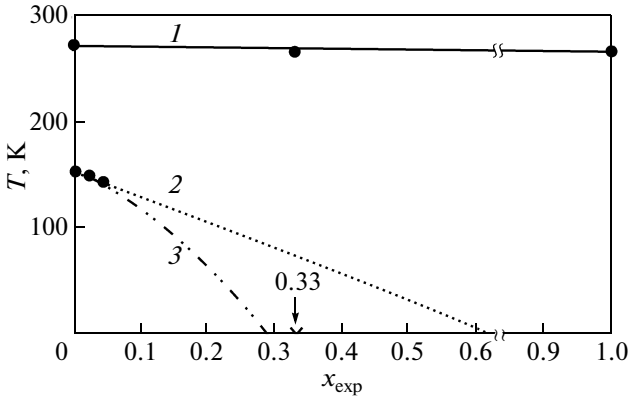

Fig. 4. Temperature–concentration phase diagram for the system of $Rb_x(NH_4)_{1-x}HSO_4$ solid solutions: (*1*) $P2_1/c$, (*2*) Pc, and (*3*) P-1 phases. The dashed line indicates the phase boundary expected from the data for x = 0–0.04. The dot-dashed line represents the conventional limitation of the existence of the P-1 phase.

Naturally, the values of the enthalpy ΔH_1 = 255 J/mol and entropy ΔS_1 = 1.1 J/mol K also appeared to be smaller than those previously determined for the compounds NH_4HSO_4 (ΔH_1 = 400 J/mol and ΔS_1 = 1.7 J/mol K) and $RbHSO_4$ (ΔH_1 = 340 J/mol and ΔS_1 = 1.6 J/mol K) [10, 13].

The search for the heat capacity anomaly associated with the transition $Pc(T_2) \longrightarrow P$-1 was continued on a Physical Properties Measurement System in the temperature range 4–90 K and also did not lead to positive results. Therefore, the antiferroelectric phase P–1 in the $Rb_{0.33}(NH_4)_{0.67}HSO_4$ solid solution is absent.

The intensive electrocaloric effect in the $Rb_{0.33}(NH_4)_{0.67}HSO_4$ solid solution in the range of the second-order phase transition was investigated under adiabatic conditions according to the technique used in the study of the NH_4HSO_4 compound in our previous work [9]. The measurements were performed in the constant electric field E = 3.4 kV/cm at temperatures in the range 240–310 K and under isothermal conditions at T = 269 K by varying the field in the range E = 0–5 kV/cm. It was revealed that the conductivity of the solid solution sample is comparable to that of the NH_4HSO_4 compound [9]. This is evidenced by an increase in the rate of variation in the temperature of the sample at $E \neq 0$ as compared to that at $E = 0$ due to the release of the Joule heat at its internal resistance. Despite this fact, the reversibility of the electrocaloric effect appeared to be rather high: the difference between the variations in the sample temperature ΔT_{ad} when switching on and switching off the electric field was within the limits of the error in the measurements.

The results of the measurements of the electrocaloric effect are presented in Fig. 3, which, for comparison, also shows the data for the NH_4HSO_4 compound. The difference between the maximum values of ΔT_{ad} for both crystals is associated with the difference between the strengths of the electric fields used in the experiments. The reduced magnitudes of the intensive electrocaloric effect $\Delta T_{ad}/E$ turned out to be rather close: 0.016 K cm/kV for NH_4HSO_4 and 0.012 K cm/kV for $Rb_{0.33}(NH_4)_{0.67}HSO_4$.

The rate of variation in the magnitude of the intensive electrocaloric effect for $Rb_{0.33}(NH_4)_{0.67}HSO_4$ in the isotherm remains almost constant $d(\Delta T_{ad})/dE \approx$ 0.06 K cm/kV (see the inset to Fig. 3) at least to field strengths of 5 kV/cm.

4. ANALYSIS AND DISCUSSION OF THE RESULTS

The calorimetric data on the influence of cation substitution on the phase transition temperatures T_1 and T_2 for a number of $Rb_x(NH_4)_{1-x}HSO_4$ solid solutions were used to construct the temperature–concentration phase diagram (Fig. 4).

For the crystals with x = 0 and 1 [10], the temperatures of the transition $P2_1/c \longrightarrow Pc$ differ by only 7 K. Since the ionic radii of rubidium and ammonium are very close to each other, there is no question that the $Rb_x(NH_4)_{1-x}HSO_4$ compounds form a continuous series of solid solutions and, hence, according to the Vegard's rule [14], the phase boundary is characterized by the coefficient $dT_1/dx \sim 0.07$ K/%. The expected transition temperature T_1 = 269.3 K for the sample with x = 0.33 agrees satisfactorily with a temperature of 269.0 ± 0.2 K for the maximum of the derivative dC_p/dT, which in our work was chosen as the temperature of this transformation (see Section 3).

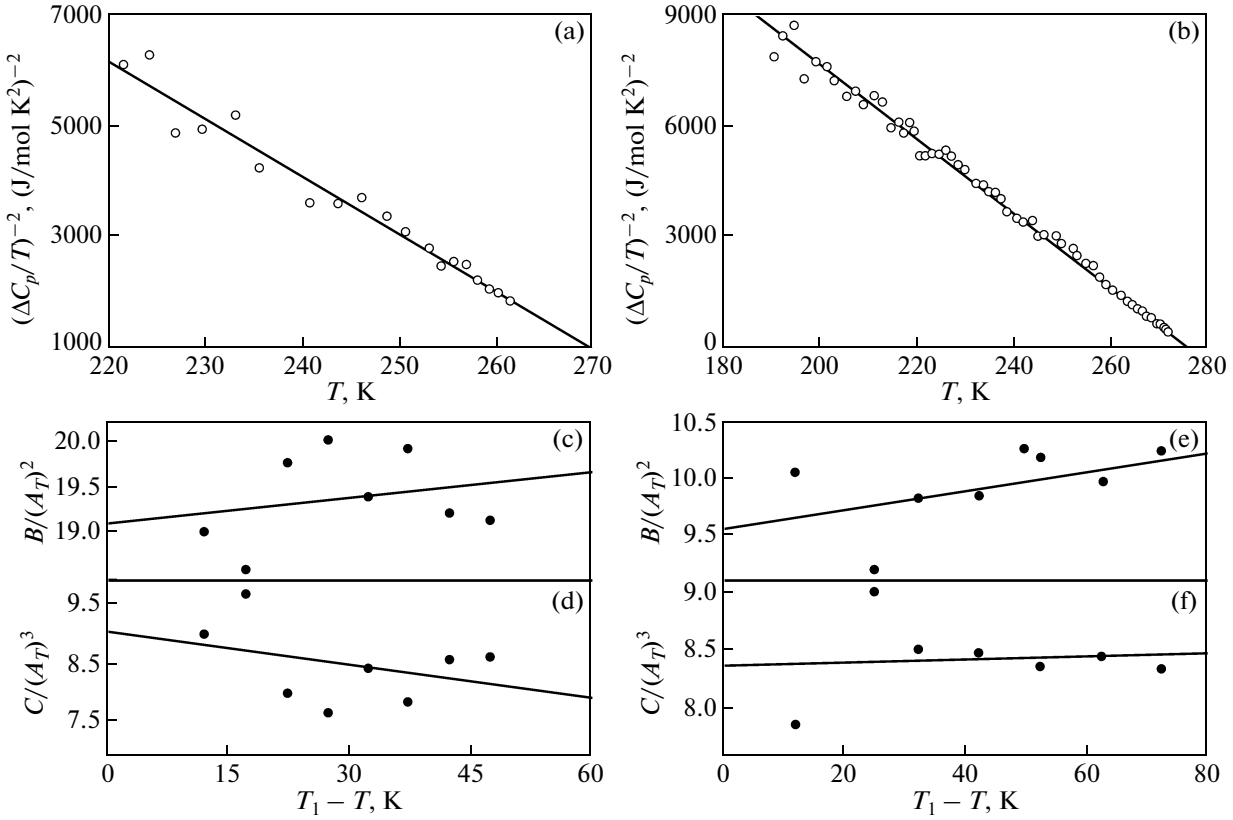

Fig. 5. Temperature dependences of the square of the inverse excess heat capacity for (a) $Rb_{0.33}(NH_4)_{0.67}HSO_4$ and (b) NH_4HSO_4. Dependences of the ratio of the coefficients (c, e) $B/(A_T)^2$ [(J/ mol K^2)$^{-1}$] and (d, f) $C/(A_T)^3$ [(J/ mol K$^{3/2}$)$^{-2}$] on $\Delta T_L = T_1 - T$ for (c, d) $Rb_{0.33}(NH_4)_{0.67}HSO_4$ and (e, f) NH_4HSO_4.

According to the established linear decrease in the temperature T_2 for samples with small values of x, the phase transition $Pc \longrightarrow P\text{-}1$ in the $Rb_{0.33}(NH_4)_{0.67}HSO_4$ sample could be expected in the range of ~80 K. However, as was noted above, no heat capacity anomalies were revealed down to liquid-helium temperatures. Therefore, the dependence $T_2(x)$ in the T–x diagram is conventionally shown in the form of a nonlinear interface (Fig. 4).

In [15], it was demonstrated that the behavior of the anomalous heat capacity in the ferroelectric phase of the NH_4HSO_4 crystal is satisfactorily described in the framework of the Landau theory in a temperature range ~(T_1 – 10 K). The representation of the excess heat capacity for the $Rb_{0.33}(NH_4)_{0.67}HSO_4$ solid solution according to the equation $(\Delta C_p/T)^{-2} = 4B^2/(A_T)^4 + 12C(T_1 - T)/(A_T)^3$ following from the thermodynamic potential $\Delta\Phi = A_T(T - T_1)P^2 + BP^4 + CP^6$ shows that the linear dependence $(\Delta C_p/T)^{-2}(T)$ is observed over a significantly wider range of temperatures, namely, ~(T_1 – 40 K) (Fig. 5a). In view of the last circumstance, we decided to newly analyze the heat capacity of the NH_4HSO_4 compound with due regard for the data obtained in [10] and using the aforementioned approach to the separation of the lattice and anomalous contributions to the total heat capacity of the crystal. It turned out that, in this case, too, the square of the inverse excess heat capacity is proportional to the temperature over a considerably wider range of temperatures in the ferroelectric phase: ~(T_1 – 80 K) (Fig. 5b). In order to verify the influence of the temperature range $\Delta T_L = T_1 - T$ included in the analysis on the parameters of the equation $(\Delta C_p/T)^{-2}(T)$, we fixed the data nearest to T_1 and varied the lower temperature limit. This procedure allows one to optimally determine the reliable range of temperatures in which the thermodynamic theory can be applied. A variation in the temperature range ΔT_L over a wide range is accompanied by a variation in the ratios between the coefficients of the potential $B/(A_T)^2$ and $C/(A_T)^3$ within 5–8% for both crystals (Figs. 5c–5f).

The coefficients B and C and the parameter $N = (B^2/3A_TCT_1)^{1/2}$ characterizing the degree of closeness of the transitions to the tricritical point were calculated with the use of the coefficient A_T determined from the data on the dependence $\varepsilon(T)$ (see table). It should be noted that, despite a decrease in the quantity ε_{max} by a factor of approximately 15 for the

Some thermodynamic parameters of the phase transition $P2_1/c \longrightarrow Pc$ in the $Rb_x(NH_4)_{1-x}HSO_4$ solid solutions

x_{exp}	T_1, K	ΔT_L, K	A_T, K^{-1}	B, $(J/mol)^{-1}$	C, $(J/mol)^{-2}$	N
0.33	269	220–265	1.4×10^{-2}	4.0×10^{-3}	2.5×10^{-5}	0.24
0	271.1	190–271.7	3.0×10^{-2}	8.9×10^{-3}	2.3×10^{-4}	0.12

$Rb_{0.33}(NH_4)_{0.67}HSO_4$ sample as compared to that for the NH_4HSO_4 compound [10], the coefficient A_T decreases by a factor of only two. As can be judged from a substantial increase in the parameter N for the solid solution, the change in the internal pressure due to the cation substitution $Rb \longrightarrow NH_4$ led to a shift in the second-order phase transition $P2_1/c \longrightarrow Pc$ from the tricritical point.

The presence of the data on the coefficients of the potential allows us to construct the thermodynamic surface E–P–T by using the electric equation of state $E = 2A_T(T - T_1)P + 4BP^3 + 6CP^5$. By analyzing this surface according to the equation [16]

$$dT = -(T/C_{p,E})(\partial P/\partial T)_{p,E}dE, \qquad (1)$$

we calculated the magnitude of the intensive electrocaloric effect for the $Rb_x(NH_4)_{1-x}HSO_4$ compounds. For comparison, the calculations were also performed for the triglycine sulfate crystal with the use of the necessary data taken from [15, 17]. In this case, it was assumed that the electric field does not affect the coefficients of the potential. This is confirmed by the data for triglycine sulfate [18], which allow us to make the inference that at least the coefficient A_T in the fields $E = 0$–1.8 kV/cm is constant. The experimental temperature dependences of the quantity ΔT_{ad} and the corresponding dependences calculated for the same electric field strengths are in satisfactory agreement (Fig. 6), which strongly supports the validity of the above assumption.

The analysis of the barocaloric efficiency was performed in the framework of the approach developed in our earlier works [6, 7] with the use of the data on the heat capacity and the pressure–temperature phase diagrams for NH_4HSO_4 [10, 19] and triglycine sulfate [17, 20]. In [19, 21], it was established that the hydrostatic pressure insignificantly affects the coefficients of the thermodynamic potential. This means that, according to the relationship for the entropy of the phase transition $\Delta S = A_T P^2$ [15], its value with a change in the pressure remains almost constant.

The total entropy of ferroelectric crystals S as a function of the temperature and pressure represents the sum predominantly of the lattice (S_{lat}) and anomalous (ΔS) entropies. Relatively low pressures ($p <$ 1 GPa) hardly affect the lattice entropy S_{lat} and, according to dT/dp, lead to a shift in the transition temperature and correspondingly ΔS in the dependence $S_{lat}(T)$. The magnitude of the extensive barocaloric effect is determined as the difference between the total entropies under pressure and without pressure $\Delta S_{BCE}(T, p) = S(T, p \neq 0) - S(T, p = 0)$ at a constant temperature.

The temperature dependences of the quantities $S(p = 0)$ and $S(p \neq 0)$ in the range of the transition $Pc \longrightarrow P\text{-}1$ in the NH_4HSO_4 compound are plotted in Fig. 7. It is evident that, in the limit, the quantity ΔS_{BCE} tends to the entropy of the phase transition,

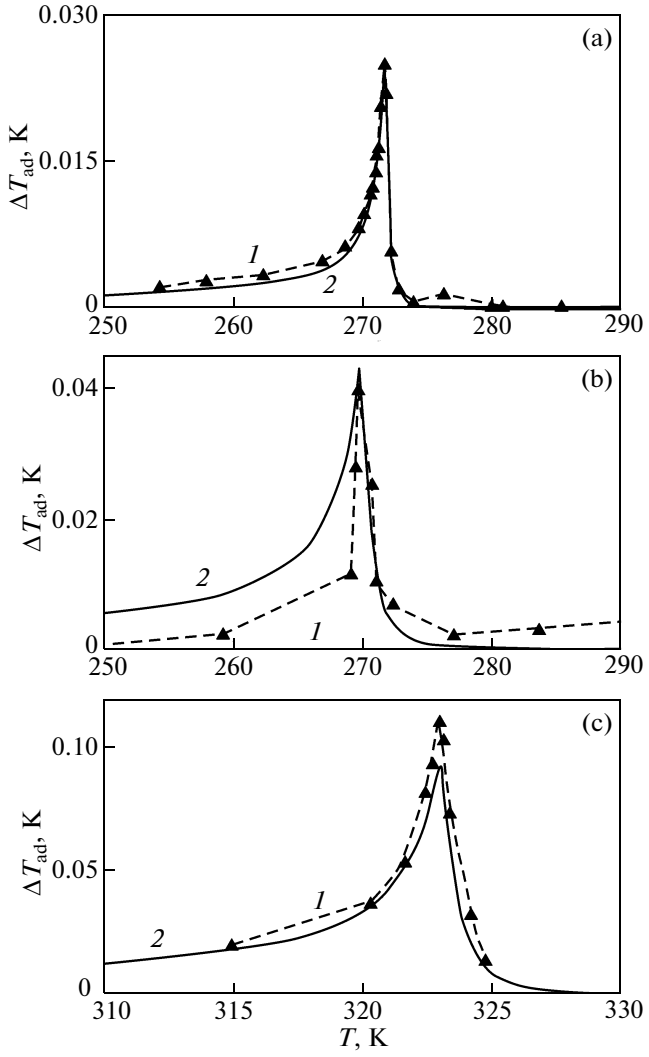

Fig. 6. (*1*) Experimental and (*2*) calculated magnitudes of the intensive electrocaloric effect for (a) NH_4HSO_4 ($E =$ 1.5 kV/cm), (b) $Rb_{0.33}(NH_4)_{0.67}HSO_4$ ($E = 3.4$ kV/cm), and (c) triglycine sulfate ($E = 1.6$ kV/cm).

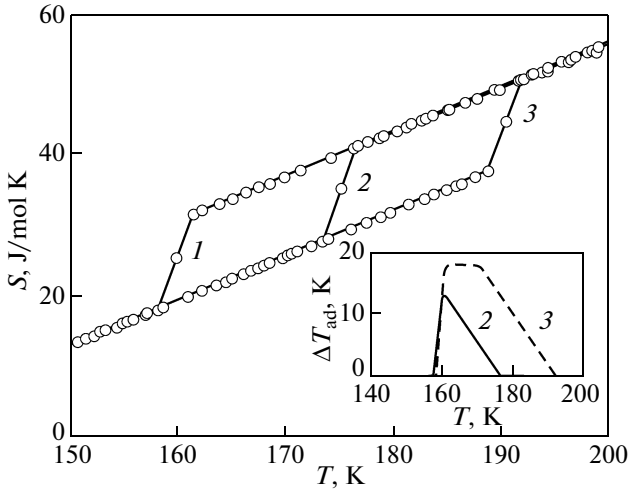

Fig. 7. Temperature dependences of the total entropy and the magnitude of the intensive barocaloric effect ΔT_{ad} (in the inset) in the vicinity of the transition $Pc \longrightarrow P\text{-}1$ for the NH_4HSO_4 compound at pressures of (*1*) 0, (*2*) 0.02, and (*3*) 0.04 GPa.

which is rather high (~Rln1.1) according to the data obtained on the adiabatic calorimeter [10].

The magnitude of the intensive barocaloric effect was also determined from the dependence $S(T)$ as a change in the temperature in the isentrope at a specific pressure. The temperature dependences $\Delta T_{ad}(T)$ are represented in the form of isobars in the inset to Fig. 7. The maximum value of $\Delta T_{ad} \approx 19$ K for the transition $Pc \longrightarrow P\text{-}1$ in the NH_4HSO_4 compound is rather large and, what is very important, is observed at very low pressures $p \geq 0.03$ GPa. Both circumstances are determined, to a considerable extent, by the anomalously large shift in the temperature T_2 for the NH_4HSO_4 compound under pressure: $dT_2/dp \approx 750$ K/GPa [19]. Therefore, according to the parameter ΔT_{ad}, the ammonium hydrosulfate compares well with many solid-state refrigerants that undergo ferromagnetic and ferroelectric phase transitions [3].

According to low entropies for the second-order transitions to the ferroelectric phase in NH_4HSO_4 and triglycine sulfate, the quantities ΔT_{ad} also appear to be insignificant and equal to 0.45 and 0.14 K at $p =$ 0.04 GPa, respectively. Although the barocaloric and electrocaloric effects have different natures, we determined the pressures leading to the same values of ΔT_{ad} that were caused by the electric fields. The value of $\Delta T_{ad} = 0.025$ K for the NH_4HSO_4 compound corresponds to $E = 1.5$ kV/cm and $p = 0.002$ GPa, and the value of $\Delta T_{ad} = 0.120$ K for the triglycine sulfate crystal corresponds to $E = 1.6$ kV/cm and $p = 0.032$ GPa. It is clear that, at the same pressure, the barocaloric efficiency of the NH_4HSO_4 compound for the ferroelectric transitions under consideration is severalfold higher.

5. CONCLUSIONS

Thus, we have investigated the influence of replacement of tetrahedral ammonium cations by spherical rubidium cations in the $Rb_x(NH_4)_{1-x}HSO_4$ solid solutions and constructed the temperature–concentration phase diagram, which indicates that, already at $x = 0.33$, the transition to the antiferroelectric phase is absent.

The behavior of the heat capacity in the ferroelectric phase and agreement between the experimental magnitudes of the electrocaloric effect and those calculated from analyzing the electric equation of state suggest that the Landau theory is applicable to the description of properties of the solid solutions over a wide range of temperatures.

The barocaloric efficiency of ferroelectric crystals has been analyzed for the first time. This analysis has demonstrated that, even for phase transitions with insignificant changes in the entropy, relatively low pressures can induce a substantial intensive caloric effect.

ACKNOWLEDGMENTS

We would like to thank A.V. Kartashev for the measurement of the heat capacity on the Physical Properties Measurement System.

This study was supported by the Russian Foundation for Basic Research (project no. 09-02-98001-Sibir') and the Council on Grants from the President of the Russian Federation for the Support of Leading Scientific Schools (project no. NSh-4645.2010.2).

REFERENCES

1. A. M. Tishin and Y. I. Spichkin, *The Magnetocaloric Effect and Its Applications* (Institute of Physics, Bristol, United Kingdom, 2003).
2. Yu. V. Sinyavskii, Khim. Neft. Mashinostr., No. 6, 5 (1995).
3. I. N. Flerov, Izv. St. Peterb. Univ. Nizkotemp. Pishchevykh Tekhnol., No. 1, 41 (2008).
4. A. S. Mischenko, Q. Zhang, J. F. Scott, R. W. Whatmore, and N. D. Mathur, Science (Washington) **311**, 1270 (2006).
5. K. A. Müller, F. Fauth, S. Fischer, M. Koch, A. Furrer, and Ph. Lacorre, Appl. Phys. Lett. **73**, 1056 (1998).
6. M. V. Gorev, I. N. Flerov, E. V. Bogdanov, V. N. Voronov, and N. M. Laptash, Fiz. Tverd. Tela (St. Petersburg) **52** (2), 351 (2010) [Phys. Solid State **52** (2), 377 (2010)].
7. M. V. Gorev, E. V. Bogdanov, I. N. Flerov, A. G. Kocharova, and N. M. Laptash, Fiz. Tverd. Tela (St. Petersburg) **52** (1), 156 (2010) [Phys. Solid State **52** (1), 167 (2010)].
8. S. Gama, A. A. Coelho, A. de Campos, A. M. G. Carvalho, F. C. G. Gandra, P. J. von Ranke, and N. A. de Oliveira, Phys. Rev. Lett. **93**, 237202 (2004).

9. I. N. Flerov and E. A. Mikhaleva, Fiz. Tverd. Tela (St. Petersburg) **50** (3), 461 (2008) [Phys. Solid State **50** (3), 478 (2008)].
10. I. N. Flerov, V. I. Zinenko, L. I. Zherebtsova, I. M. Iskornev, and D. Kh. Blat, Izv. Akad. Nauk SSSR, Ser. Fiz. **39**, 752 (1975).
11. S. R. Miller, R. Blinc, M. Brenman, and I. S. Wang, Phys. Rev. **126**, 528 (1962).
12. B. A. Strukov, S. A. Taraskin, and V. A. Koptsik, Zh. Eksp. Teor. Fiz. **51** (4), 1037 (1966) [Sov. Phys. JETP **24** (4), 692 (1966)].
13. I. N. Flerov and I. M. Iskornev, Fiz. Tverd. Tela (Leningrad) **18** (12), 3666 (1976) [Sov. Phys. Solid State **18** (12), 2135 (1976)].
14. L. Vegard, Z. Phys. **V**, 17 (1921).
15. K. S. Aleksandrov and I. N. Flerov, Fiz. Tverd. Tela (Leningrad) **21** (2), 327 (1979) [Sov. Phys. Solid State **21** (2), 195 (1979)].
16. G. A. Smolenskii, V. A. Bokov, V. A. Isupov, N. N. Krainik, R. E. Pasynkov, and M. S. Shur, *Ferroelectrics and Antiferroelectrics* (Nauka, Leningrad, 1971) [in Russian].
17. B. A. Strukov, E. P. Ragula, S. V. Arkhangel'skaya, and I. V. Shnaidshtein, Fiz. Tverd. Tela (St. Petersburg) **40** (1), 106 (1998) [Phys. Solid State **40** (1), 94 (1998)].
18. I. M. Sil'vestrova, Kristallografiya **6** (4), 582 (1961) [Sov. Phys. Crystallogr. **6** (4), 466 (1961)].
19. I. N. Polandov, V. P. Mylov, and B. A. Strukov, Fiz. Tverd. Tela (Leningrad) **10** (7), 2232 (1968) [Sov. Phys. Solid State **10** (7), 1754 (1968)].
20. G. G. Leonidova, I. N. Polandov, and I. P. Golentovskaya, Fiz. Tverd. Tela (Leningrad) **4**, 3337 (1962) [Sov. Phys. Solid State **4**, 2443 (1962)].
21. G. G. Leonidova, N. P. Netesova, and T. R. Volk, Fiz. Tverd. Tela (Leningrad) **9** (2), 593 (1967) [Sov. Phys. Solid State **9** (2), 454 (1967)].

Translated by O. Borovik-Romanova